Author accepted manuscript of:
Mullings, H.R., Stallard, T., Payne, G.S (2017) Operational Loads on a Tidal Turbine due to Environmental Conditions. Paper Number 939. *Proceedings of The Twenty-seventh (2017) International Ocean and Polar Engineering Conference.* San Francisco, California, USA, June 25-30, 2017

Operational Loads on a Tidal Turbine due to Environmental Conditions

Hannah R. Mullings, Tim J. Stallard
School of Mechanical, Aerospace and Civil Engineering
The University of Manchester, Manchester
United Kingdom

Grégory S. Payne
Institute for Energy Systems,
The University of Edinburgh, Edinburgh
United Kingdom

ABSTRACT

Accurate assessment of the fatigue life of tidal stream turbines and components requires prediction of the unsteady loading of turbine components over a wide range of frequencies. This study focuses on the influence of ambient turbulence, velocity shear and the approach taken to model wave kinematics, on the variation of thrust load imposed on the rotor shaft and supporting tower. Load cycles are assessed based on sea-state occurrence data taken over a five month period for a case study site. The influence of each environmental parameter on component loading is evaluated and the impact on material design parameters assessed. Alternative approaches are considered for modelling turbulent loading and wave loading. The frequency variation of loads due to turbulence are scaled from experimental data from trials of a three-bladed horizontal axis turbine of 1.2 m diameter on a bed-mounted supporting structure. Frequency dependent wave loading is estimated by a relative form of the drag term of the widely used equation of Morison et al. (1950), with the depth decay of kinematics modelled by linear wave theory. Over the five month interval considered a ten year design life can be obtained with a lower design load by accounting for variation of turbulence intensity that occurs during each tidal cycle. This is expected to vary further with the approach taken to model the onset turbulence. A component can also be designed for lower loads over the same time period if irregular waves are modelled instead of regular.

KEY WORDS: Tidal Turbine; Fatigue; Turbulence; Waves; Damage Equivalent Loads.

INTRODUCTION

The aim of this study is to assess the relative importance of turbulence and wave-induced unsteady loading on the design life prediction for a typical horizontal axis tidal turbine. In recent years, there has been increasing interest in tidal stream turbines for large scale electricity generation. A number of devices, typically horizontal axis turbines, have now been demonstrated at full-scale and planning for deployment of small tidal arrays is ongoing for sites in the UK - Pentland Firth, (Meygen (2017)), France - Paimpol-Brehat (DCNS (2016)) and Raz Blanchard, (European Commission (2016)) as well as Canada - Bay of Fundy, (Natural Resources Canada (2016)). Design of individual turbines and turbine components relies on prediction of the cyclic loading experienced since this directly affects fatigue life, hence availability and economic viability. It is expected that commercial farms would comprise arrays of turbines (Meygen (2017)) for which the mean and unsteady loading will vary with position within the array. However when operating in widely spaced arrays, turbine loading will be similar to an isolated turbine with unsteady loads dominated by the ambient environmental conditions. The magnitude of flow shear, turbulence intensity and length scale and the kinematics induced by surface wave conditions all influence loading and can vary with flow speed and direction.

At present lifetime estimates for tidal turbine components such as blades fall short of planned maintenance schedules from developers, (Galloway (2013)). Experimental studies into the effect of loading on power and performance have been

conducted. Work has also been done to simulate turbulence and wave effects, (Gaurier et al. (2013); Blackmore et al. (2016)) and shear, (Fleming et al. (2013)). Chamorro et al. (2013) conducted a spectral analysis to determine a critical frequency below which the variation of onset flow dominates unsteady loading and above which the turbine operating point determines loading. This was found to vary linearly with angular frequency of the turbine. Experiments were carried out as part of the XMED project at the IFREMER test facility. The turbulence levels and wave conditions were similar to those studied by the IFREMER group to assess wake recovery and thrust variation of a turbine with surface piercing support (Mycek et al. (2014)) including due to waves, (Gaurier et al. (2013)). The experimental set up and design of the turbine used is given in **?**.

The intention of the present study is to estimate cyclic loading experienced by a tidal turbine over a typical operating period to assess suitability for alternative deployment locations, initially for a turbine operating in isolation and, longer term within an array. Through modelling the loads and calculating the corresponding damage equivalent loads, the importance of different environmental conditions will be assessed. For example, the accuracy to which wave conditions and turbulence conditions must be established to determine damage equivalent loads to a given accuracy will be evaluated. Key questions to be addressed include the accuracy to which wave conditions are required to determine the damage equivalent loads (DELs). Loading for a given combination of environmental conditions is estimated from a synthesised loading spectrum. Applying this approach to each sea-state experienced by the turbine provides the aggregate load cycles from which design life is inferred.

In the following sections a brief review is given, the case study environmental data described and the approach taken to obtain frequency dependence of loads due to turbulence and waves for a generic horizontal axis turbine briefly described. The subsequent results address the influence of turbulence, regular or irregular waves on load cycles and on the design parameters required to attain a nominal design life.

DESIGN LIFE PREDICTION

Initial work into establishing the fatigue life of components due to environmental conditions was conducted by McCann (2007). This study looked into the sensitivity of the fatigue life due to turbulence and waves, using the DNV-GL software Tidal Bladed. A variation of fixed flow speeds, turbulence intensities and wave conditions were used as an example of values similar to site conditions. Fatigue life was found to be highly sensitive to the variation in both wave conditions and turbulence intensities. Further work into examining the fatigue life has focussed on specific component areas which have been informed by the failures found in the wind turbine industry, (Veers (2009)). These areas were the blades (McCann (2007), Galloway (2013)) and various components within the drive train; gearbox, bearings (Val and Chernin (2011), Elasha et al. (2015)). Drawing on experience from field trials including within the ReDAPT project DNV-GL (2015) have recently published a standard for certification of horizontal axis tidal stream turbines. The standard established that fatigue test loads should be developed based upon the design spectrum.

One method for quantifying the design life is by using damage equivalent loads (DELs). The purpose of these is to help evaluate the fatigue damage which is found over a flow cycle caused by repetition of a single magnitude load at a representative frequency (McCann (2007)). This facilitates direct comparison between different unsteady loading cases. This method requires a need for a representative frequency to be used as the value at which the load repeats.

$$DEL = \left(\frac{\sum_i n_i {L_i}^m}{fT} \right)^{\frac{1}{m}} \tag{1}$$

Where L_i is the load at bin i, m is a material property given by the slope of the S-N curve for the material, T is the length of time for operation, f is the repetition frequency, n_i is the number of cycles at given load.

This method for calculating the equivalent loads has been used by Freebury and Musial (2000), in a process for calculating the number of cycles to failure with no known material or structural data for the component. This incorporates an approximation of the gradient of an S-N curve (stress/load vs number of allowable cycles) to calculate the allowable

cycles to failure using Eq. 2.

$$N_i = \left(\frac{F_A}{F_U}\right)^{-m} \tag{2}$$

Where F_A is the load amplitude for a given cycle, F_U is the ultimate load amplitude and N_i is the allowable cycles before failure. The most widely used method for calculating damage models for failure caused by fatigue is the Palmgren-Miner's rule. This is given in Eq. 3.

$$\sum_{i=1}^{I} \frac{n_i}{N_i} = D_C \tag{3}$$

Where D_C is the characteristic cumulative damage fraction and is calculated with a known number of cycles to failure (N_i) for a given load. This is usually found from an M-N curve specific to the material of the component, or Eq. 2 is used with an S-N curve. The design cumulative damage, D_D, is then found by multiplying the characteristic cumulative damage by the design fatigue factor (DFF), shown in Eq. 4.

$$D_D = DFF(D_C) \tag{4}$$

The design life, in years, can then be estimated using Eq. 5, with design life limit $C_{des} = 1$ representing the point at which failure occurs, D_D as defined by Eq. 4 and Y_f a fraction of the number of samples used within a year. This formula has been used in Galloway (2013) to predict the lifetime of blades based on the load cycles generated from in-plane and out-of-plane bending moments.

$$L_{years} = 100(Y_f)(C_{des} - D_D) \tag{5}$$

These load cycles are affected by how the turbine is controlled as well as the environmental conditions. In this paper the focus is on the affect on the load cycles of variations in environmental conditions, turbulence and waves, over multiple tidal cycles. The influence of operating mode is only briefly assessed and a short review of the types of set up which are generally used is given in the next section.

TURBINE CONTROL

Establishing the use of a horizontal axis turbine for tidal stream turbines, is an initial step into examining the device design. For the application of this style of device into a grid array, different set-up options have been explored to maximise energy production and to limit maximum loading. Following an ideal power curve there is a region where the turbine operates with available power below rated, when flow speeds are below rated, where the power coefficient (C_P) is maximum. There are two key factors which are varied to optimise the efficiency and power output, these are rotational speed of the turbine and the blade pitch. These two options are combined to give four operational set ups; fixed speed - fixed pitch (FS-FP), fixed speed-variable pitch (FS-VP), variable speed- fixed pitch (VS-FP) and variable speed-variable pitch (VS-VP), (Bianchi et al. (2006)). In terms of investigating fatigue life on a tidal turbine component the majority of work has considered environmental effects only. Here the influence of turbine operating approach, whether operating at variable or fixed speed, on the the number of load cycles is also considered.

ENVIRONMENTAL CONDITIONS

Three environmental conditions will be examined in this case to determine the affect on load cycles and hence on damage equivalent loads (DELs) and on design life. These are the velocity profile, turbulence and waves. The period of each wave along with the direction and relative height are important in determining the affect of waves on blade loads. Waves can enhance turbulent loads, and this can govern the design life of the blade, (Milne et al. (2010)). Accurate prediction of wave-induced loads is however not trivial, particularly over the broad range of heights and frequencies, each with differing depth decay through a typically sheared onset flow.

A location in the Pentland Firth is considered as an example site. Mean flow speed at ten minute intervals, is modelled by a nine tidal constituent model. Nine tidal constituents have been used as they had the largest amplitude peaks from

analysis of other models, as a close approximation to the time series modelled in an ocean circulation model (ADCIRC, **?** and **?**). Wave data was provided by the Environmental Research Institute and The University of Highlands and Islands, Thurso, from a six month deployment of a Datawell directional waverider buoy MKIII. Five months of data is used here from mid-January to mid-June. The data collected was sampled every 30 minutes, this was then interpolated using linear interpolation to give a measurement every 10 minutes. This rate of sampling environmental data is used throughout the DNV-GL standard when determining loads, DNVGL-ST-0164 (DNV-GL (2015)). The significant wave height and peak period have been used in this analysis as the key identifiers to inform the types of waves, as used in McCann (2007). Fig. 1 shows the variation in significant wave height in metres, this variation is used completely in the load cycle analysis. However at certain conditions, $H_S > 3$ m, the turbine would cut out and stop rotating to reduce load, so the impact of this cut off parameter is examined to determine any affect on the number of load cycles. The peak period is given in Fig. 2.

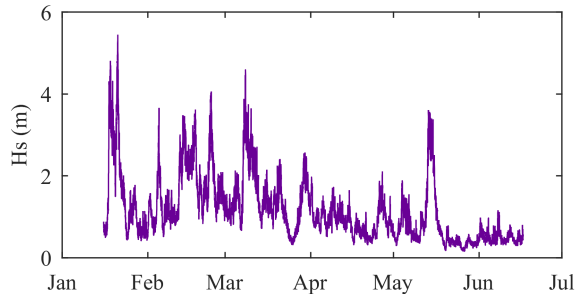

Fig. 1 Significant wave height variation over five months

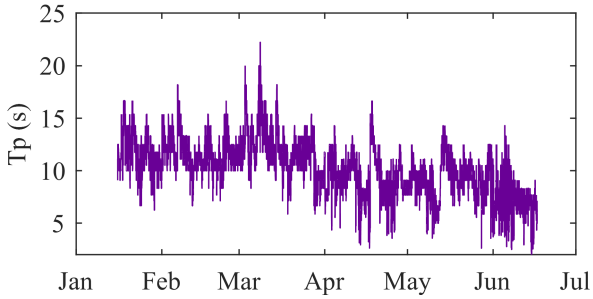

Fig. 2 Peak wave period variation over five months

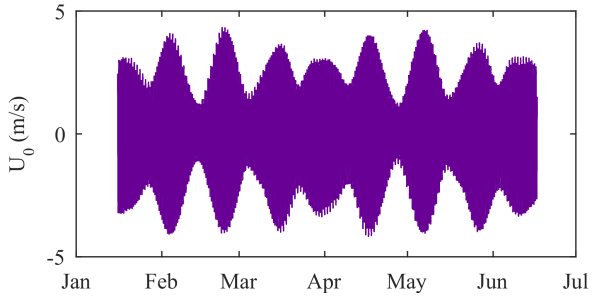

Fig. 3 Flow variation over five months

Kinetic energy spectra during each ten minute interval is estimated based on the flow-speed and turbulence intensity. Five months of this model has been used for direct comparison with the five months of usable wave data obtained, Fig. 3.

PREDICTING LOAD CYCLES

The number of load cycles over multiple tidal-cycles is an aggregate of the unsteady loading during each of the quasi-steady intervals which occur, each characterised by flow speed, wave height, period and turbulence intensity. The number of quasi-steady intervals depends on the location, as well as the sample size. In this case the Pentland Firth is considered with the obtained resource data summarised in the previous section. The spectrum of loading differs in each quasi-steady ten-minute interval and this is approximated by combinations of the following cases:

1. Establish the turbulent loading due to intensity variation, through spectral analysis.
2. Establish loading due to waves at the peak wave frequency.
3. Establish affect of shear on operational peaks, caused by control methods.

These three cases are used to give prediction of load cycles to calculate damage equivalent and ultimate loads for a given design lifetime.

Spectrum of Loads due to Turbulence

This load spectrum has been scaled from experimental measurement of thrust force at a given environmental condition from the XMED tests, (**?**). For this study the load spectrum used is from a 3% turbulence intensity case with no waves present and free stream velocity of 0.8137 m/s. The spectrum is shown in Fig. 4.

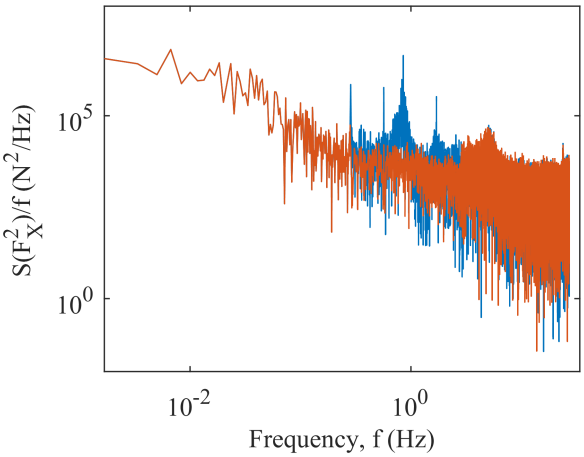

Fig. 4 Original load spectrum (-) and new approximate spectrum (-)

When examined the peaks present are caused by shear and tower loads, at frequencies corresponding to harmonics of the turbine rotational frequency. To develop a generic load spectrum which is used as an approximate spectrum for a range of sea states and operating parameters the peaks present are filtered out. This is done over the range of frequencies affected by the operating and environmental conditions ($f_0 - 10f_0$). The filtered spectrum is shown by the orange line in Fig. 4. A low order median filter was applied to remove the narrow peaks from the data, the data was then normalised using a coarse windowed spectrum and then adjusted to the overall trend found in the specified frequency range by the use of a high order median filter. The measured spectrum is from a device $1/15^{th}$ of full scale, therefore the spectrum of rotor thrust is scaled accordingly, using Froude scaling, to provide an approximate full scale load spectrum. Between the approximate and original spectrum there is only a 1.1% difference in total number of load cycles. This difference is considered negligible and this approach is used to determine range of load cycles over numerous sea states and operational conditions.

Turbulence Loading

Taking an average profile of the turbulent trends from the three different measuring devices in Sutherland et al. (2012), a relationship between turbulence intensity and flow speed is found. This relationship is shown in Fig. 5.

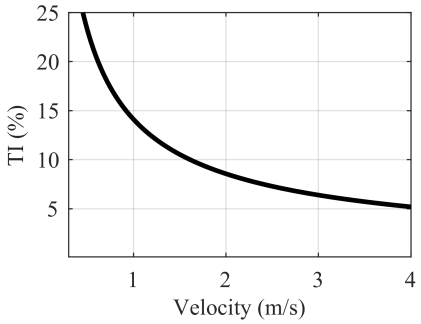

Fig. 5 Averaged relationship between flow speed and turbulence intensity

Using the flow speeds from the tidal constituents model the turbulence intensities are determined over the same interval. At lower flow speeds (U_0<0.5 m/s) the TI tends to increase dramatically, therefore a cut off value has been used of 23.3% for all flow speeds below 0.5 m/s. The values of turbulence intensity over the same five months as the flow speed are shown in Fig. 6.

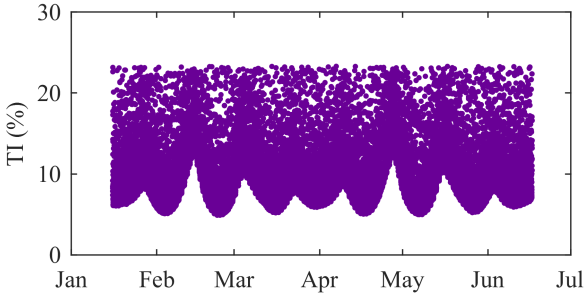

Fig. 6 Turbulence intensity variation

This variation is used in conjunction with the flow speed variation on an approximate load spectrum, to determine the effect of the variation within a model onto the design life. By increasing the y-intercept of the spectrum relative to the TI and mean velocity squared. This spectrum then has an inverse Fourier transform applied with random phase to convert the data back into the time domain for applying the Rainflow analysis (Downing and Socie (1982)), which determines the cycle range and number of cycles each range.

Wave Loading

The maximum force in the presence of a current is approximated by superposition of a wave induced force and a current induced thrust force, (Fernandez-Rodriguez et al. (2014)), Eq. 6.

$$F_M = \frac{1}{2}\rho A_s (C_{D,W} U_W^2 + C_T U_C^2) \tag{6}$$

Where A_S is the swept area of the rotor, $C_{D,W}$ is the drag coefficient of the wave, in this formulation $C_{D,W} = 11$, Fernandez-Rodriguez et al. (2014), in agreement with drag coefficients obtained for a flat-plate in planar flow at similar Keulegan Carpenter number by **?**, U_W is the wave velocity, C_T is the thrust/drag coefficient induced by the current, gathered from C_T(TSR) curves for the device, U_C is the current velocity. A comparison between the experimental peaks found from three XMED tests with waves, and the wave induced force is shown in Table 1. This shows agreement within 10% for the peak thrust.
However due to the U_W^2 term Eq. 6 only provides the maximum force for a given wave condition, whereas the time variation is required to obtain load cycles. To obtain the amplitude of fluctuation around a long run mean, the following relative form of the Morison et al. (1950) formulation, Eq. 7, is used, this follows the approach of **?** and has been evaluated

Table 1 Comparison of forces

Wave Case	F_M (N)	Experimental Peak (N)	% Difference
Case 1	354.5963	321.1289	9.4%
Case 2	357.8118	340.0708	5.0%
Case 3	357.4745	342.6661	4.1%

for porous disc loading due to current and waves by Fernandez-Rodriguez (2015).

$$F_M = \frac{1}{2}\rho A_s C_{D,W} U_W |(U_C - U_W)| \tag{7}$$

Herein U_W refers to the disk averaged velocity over the rotor plane. Calculated by splitting the rotor area into sufficient number of horizontal segments, determining the area of each segment and multiplying by the horizontal velocity at the mid-point of that segment. This wave-induced velocity is obtained for an irregular wave assuming linear wave theory:

$$u_{wave}(z,t) = \sum_{i=1}^{N} \left(\frac{\pi 2a(f_i)}{T_P} \frac{\cosh(k_i(d+z))}{\sinh(k_i d)} \right) \cos(\phi_i - \omega_i t) \tag{8}$$

Where d is the total water depth, k is the wave number satisfying the linear dispersion relationship, neglecting Doppler shift of the frequency due to the current. There are N discrete frequency values $i = 1 : N$ and t the time. In this case $N = 100$ but can be any arbitrarily large number. For a regular wave, $N = 1$ and $z = d/2$. For irregular waves, $N = 100$ but can be any arbitrarily large number. The amplitude of each component frequency f_i is determined by Eq. 9.

$$a(f) = \sqrt{2 S_{PM}(f) df} \tag{9}$$

These amplitudes are found at prescribed discrete frequencies over a range which includes the f_p for each wave peak, where $df = 2.5 f_p / N$. The amplitude of each component is determined assuming a Pierson Moskowitz spectrum:

$$S_{PM} = \frac{H_s^2}{4f} \left(\frac{5 f_p^4}{4 f^4} \right) e^{-\frac{5 f_p^4}{4 f^4}} \tag{10}$$

Taking Eq. 8 as input to Eq. 7 provides a force time history for irregular wave force on the disc. This is then superposed with the time history of force due to turbulence and shear and this aggregate force analysed to obtain the overall number of cycles and range.

Periodic Loading

This loading occurs at rotor operational frequencies and is mainly created from shear loading and loading caused by tower shadow. Shear loading considered in this case, is in the vertical plane and is created by the surface roughness and boundary layer at the seabed. This supplies an opposing shear force to the flow at the bed and hence a a non-uniform flow from the sea surface to the bed. Due to operating restrictions, shipping channels, tidal turbines would typically be in the lower half of the vertical column, hence the effect of shear can be quite significant. This is modelled using a blade element code, in this case Tidal Bladed has been used to assess the mean force on the rotor and the influence of different shear profiles. Using Eq.11 the trend between amplitude and power law index has been determined for a turbine sitting at the same position in a flow, using the same approximate depth of water as the Pentland Firth. For simplicity, in this case a constant shear profile was applied using a $1/7^{th}$ index, which has been measured at full scale tidal sites, (Sutherland et al. (2012)).

$$\Delta F_S = 0.033 PLI^2 - 0.0023 PLI + 0.001 \tag{11}$$

Where PLI is the power law index. The total magnitude of the shear force is calculated using the amplitude, ΔF_S, in addition to the mean thrust force, F_X found for each 10 minute interval over the 5 month period. The variation in operating point then determines the frequency at which the shear force is then applied to the load spectrum. With the frequencies differing depending on whether it is a fixed or varying operating point, rotational frequency. Tower shadow also affects the magnitude of the periodic loading at the rotational frequencies and studied by Parkinson and Collier (2016), however that effect has not been included in this analysis.

Operating Conditions

The choice of operating a turbine at fixed or variable speed affects the frequency location of the peaks within the loading spectrum. For a variable speed turbine the site flow speed dictates the position of the turbine operation on the power curve hence C_P. Using C_P and an appropriate C_P(TSR) curve the range of operating TSRs are found. This allows the variation in C_T to be found using a C_T(TSR) and hence mean force acting upon the rotor, F_X.

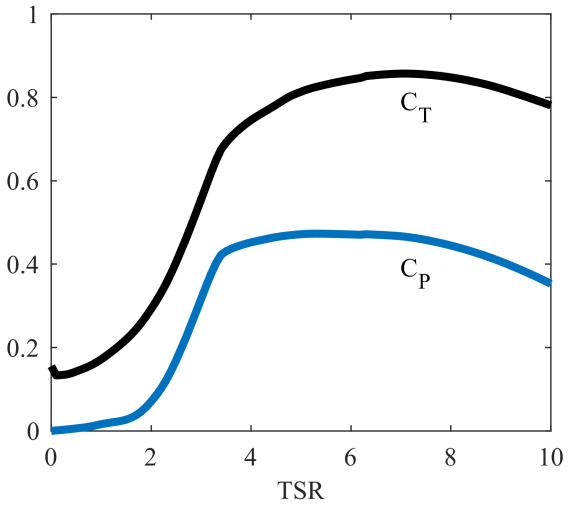

Fig. 7 C_P(TSR) and C_T(TSR) curves for a full-scale turbine

For a fixed speed turbine the rotor speed is arbitrarily chosen as a peak value of C_P which produces a plateau on the power curve at the design rated power. In this case a C_P of 0.38 has been chosen as it limits the power of this example full-scale turbine to 1MW. Using this C_P the TSR is found using the same C_P(TSR) curve as used for the variable speed turbine and shown in Fig. 7. The flow speed which gives rated power at the chosen C_P is then used with the TSR to give the fixed rotational speed. Using the five months of flow data and this fixed speed the variation of TSR is found as well as the variation of C_P and C_T. Hence the variation of mean force F_X which allows the magnitude of shear to be applied, at the operational frequency which corresponds to the fixed speed.

RESULTS AND DISCUSSION

Different parameters have been used to assess the affect of conditions and approach on the loads experienced by turbine components. In this study the thrust force on the rotor has been used as the load case. Eq.3 has been used to calculate the damage fraction which allows the design life to be found using Eq.5. For a component such as the drive shaft to be designed for a specified design life before maintenance, the damage fraction, with the included design fatigue factor is calculated. This allows an estimate of the required ultimate load for a given material to be identified. Here a design life of ten years is considered. Comparing a variety of different modelling approaches, it is then used to assess the importance of the influence of the conditions and methods. The damage equivalent loads included here have been calculated using Eq.1. With the representative period taken from the weighted average number of cycles within the five month period and for the same design life. A comparison has been made between the use of different materials defined by the use of the material gradient which is taken from a Wöhler's curve.

Influence of Turbulence

A range of turbulence cases have been evaluated; four constant intensity sets and one using the variable intensity established in Fig. 6. Using a cut off of $U_0 < 0.5$ m/s every quasi-steady spectrum which represented that case has been ignored in the calculation of the load cycles. Fig. 8 shows the number of load cycles at each range calculated from the Rainflow analysis of the multiple time series. Included on this graph is the plot of the approximate M-N curve of the component at

a certain condition, calculated using Eq. 2 with the ultimate load taken for a target design life of 10 years, with material gradient $m = 10$, using the 10% turbulence case as an example.

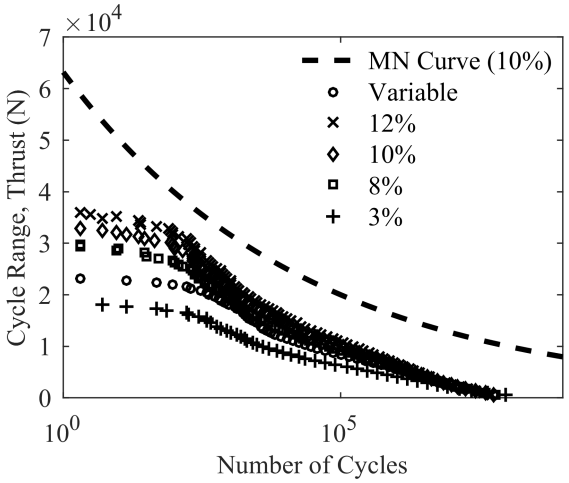

Fig. 8 Range and number of load cycles over the 5 months, with differing assumptions on turbulence intensity

For each turbulence case the maximum environmental load is obtained using the range and mean from each cycle determined from the Rainflow analysis. The DELs with the period at which they occur and ultimate loads are presented for both material properties in Table 2.

Table 2 Comparison of alternative turbulence intensities and material properties

TI	Env. load, F_{max} (kN)	Damage equivalent load Period (s)	(kN)		Ultimate load, F_U (kN)	
			$m = 4$	$m = 10$	$m = 4$	$m = 10$
3%	8.4	2.7	2.1	5.2	319	39
8%	13.7	1.1	3.3	8.5	510	64
10%	15.3	1.4	3.6	9.3	567	71
12%	16.8	1.3	3.9	10.1	628	78
Variable	10.7	1.7	3.1	7.2	456	48

A decrease in ultimate load is found from the 12% to 3% turbulence cases which is expected as the fluctuations decrease around the mean. For the variable case the ultimate load is greater than the 3% case but less than the 8% case. This is due to the minimum TI for the variable case being 4.9% so much larger fluctuations are found at all points compared to the 3%, mean TI for the variable case is 8.9% but overall a smaller range across the five months than a constant TI at 8%. This study highlights the affect of assuming constant TI instead of actual varying TI. The peak environmental load range found for the 12% and variable case occurs at the highest current flow speed of 4.34m/s, this could be considered as another shut down criteria. However the peak force found for the variable is at a TI of 4.9% which causes the reduction in peak compared to the 12% case.

The damage equivalent loads found for each material case match the trend presented by ultimate loads, with the lower turbulence cases having lower damage equivalent loads. The damage equivalent loads have also been compared between the two material cases. The results show that for the same cyclic time period in both cases the more flexible material, m= 10, have greater DEL than the stiffer case, $m = 4$. This trend corresponds with the results found for the blade moment loads in McCann (2007). The ultimate load for steel, $m = 4$, is significantly greater than the for the case where the material is slightly more flexible, $m = 10$. This is due to the volume of cycles around the mid cycle load range which for the steeper, $m = 4$, produces a damage fraction much greater than 1.

Influence of Waves

The inclusion of waves into each quasi-steady spectrum uses the significant wave height (H_s) and time period (T_P) over the five months. Within this period of time the Hs has been measured over 3m, which now means a cut off is included, by ignoring the load cycles found at every spectrum where $H_s > 3$ m. Initially the waves have been included as a peak force combined with the turbulent spectrum at the desired wave frequencies, these are henceforth referred to as regular waves. The number of cycles at each cycle range is shown in Fig. 9 for both with and without cut off.

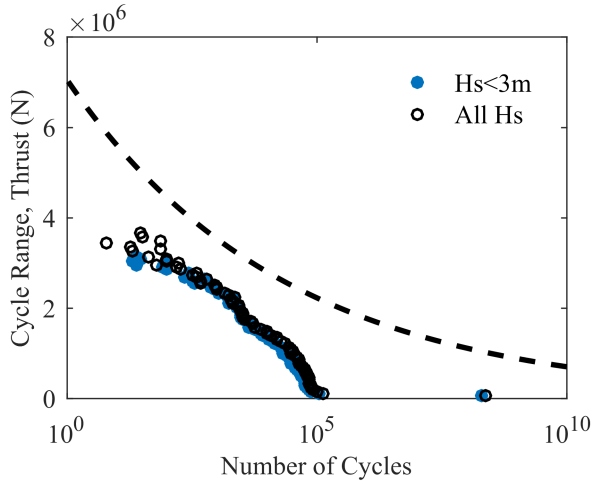

Fig. 9 Load cycles for 5 months with variable turbulence and regular waves with and without the, H_s and U_0 cut off criteria

Fig. 9 shows a slight difference in the peak cyclic range between the two cases. At each range there slightly more cycles included, this is due to the cut off criteria removing the number of cycles for those cases where $H_s > 3$ m. The contribution of the turbulence is clearly seen by the points found at the minimum range and with number of cycles greater than 10^5.

A comparison has been made between number of cycles and magnitude of those cycles with and without the cut off, Table 3. By introducing the cut off there is no change in the environmental load range for the regular wave case, as highest applied force is found at a $H_s = 1.41$ m, so below the cut off limit. By including the cut off the DEL reduces but with smaller period, hence greater cycles over the design life. When compared with the variable turbulence only case, the ultimate load is found to have increased, this is due to the implementation of the calculated thrust force due to the wave at the wave frequency being much larger than the force caused by the turbulence that it replaced. The peak wave force is found at a flow speed 4.13 m/s and a low TI of 5.1%.

Table 3 Comparison of Loads for Both Wave Cases

	Waves	Env. load, F_{max} (kN)	Damage equivalent load Period (s)	(kN) m= 4	m=10	Ultimate load, F_U (kN) m=4	m=10
Regular	All H_s	1822	15.8	540	1253	46215	7616
	$H_s < 3$m	1569	13.3	487	1182	43283	7138
Irregular	All H_s	1286	5.5	387	1098	43155	7261
	$H_s < 3$m	965	4.8	285	770	24633	5161

For each wave case with and without cut off, the affect of including the wave as an irregular instead of regular wave is found. This utilises the Pierson Moskowitz spectrum shown earlier in Eq.10 to determine a range of thrust force over time which is then combined with the variable turbulence case. The environmental, damage equivalent and ultimate

loads for the irregular case are also given in Table 3. It is clear that including the variation of rotor thrust using the time varying approach produces much greater range of environmental load. However by including the cut off criteria there is a reduction in the maximum environmental load. This is located at a H_s = 4.03 m and therefore not included in the limited case, which can be seen on Fig. 10.

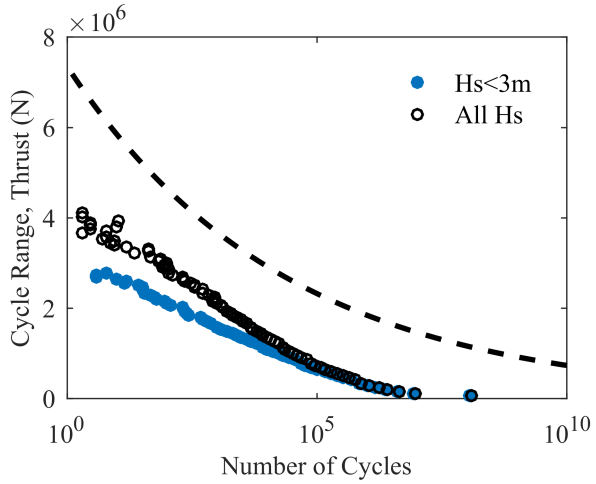

Fig. 10 Load cycles for five months with variable turbulence and irregular waves, with and without the, H_s and U_0 cut off criteria

The damage equivalent loads for the irregular case match the same trend as those seen for turbulence in which using a material property of m = 4 produces a lower DEL than when m = 10. The introduction of the cut off shortens the period of the DEL as well as reducing the magnitude. The ultimate loads for the irregular wave cases are much greater than the damage equivalent loads as these loads can only occur once to provide a lifetime of 10 years. There is a noticeable difference in the gradient of the points for each wave case. The regular wave case provides a much higher frequency of occurrence for any cycle range greater than 0.5 MN than the irregular wave cases. This leads to much higher ultimate loads with respect to the irregular case for environmental loads which are similar. It can be seen that regardless of technique used to generate the wave forces, loads due to waves dominate over loads due to turbulence, but inclusion of the cut off reduces the load that the component should be designed to last under.

Influence of Shear

Using the mean thrust force, F_X, and the variation defined by Eq. 11, the peak amount of shear is applied for each 10 minute interval. The variation in operating point then determines the frequency at which the shear force is then applied to the load spectrum. With the frequencies differing depending on whether its a fixed or varying operating point, rotational frequency. The shear comparison cases are combined with the variable turbulence, as with waves, to establish the effect of shear. The various calculated loads are given in Table 4.

Table 4 Comparison of loads considering turbulence and shear

	Env. load, F_{max} (kN)	Damage equivalent load Period (s)	(kN)		Ultimate load, F_U (kN)	
			m = 4	m = 10	m = 4	m = 10
Turbulence Only	10.7	1.7	3.1	7.2	456.0	48.0
Turbulence +(1)	10.9	1.7	3.1	7.2	457.7	47.1
Turbulence +(2)	11.0	1.7	3.1	7.2	458.0	47.7

(1) = shear applied at fixed operating point,
(2) = shear applied at variable operating point

It can be seen that the influence of shear is negligible with slight changes in the ultimate load which corresponds to the

differences found in the environmental load. The damage equivalent loads for each case and each material property show no variation, even though Fig. 11 shows slight change in the number of load cycles at higher cyclic ranges.

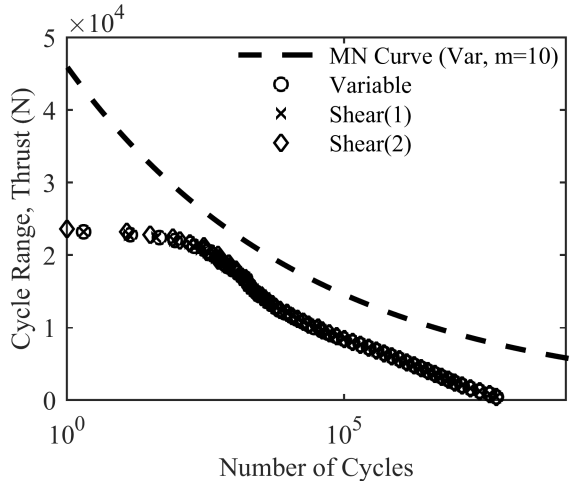

Fig. 11 Load cycles for five months with variable turbulence and (1): shear (fixed), (2): shear (variable)

The influence of shear has little impact on the magnitude of the load range from the variable turbulence case. Therefore to examine the combined affect only one of the two operating cases is used, the variable operating point due to the environmental load being slightly higher.

Combined Environmental Loads

A comparison of the influence of the different environmental and operating conditions is performed using the various load calculations as in the previous sections. Continuing with the variable turbulence case and shear applied at a variable operating point, the effect of the three different wave conditions are compared, Table 5.

Table 5 Comparison of loads considering turbulence, shear and waves

	Env. load, F_{max} (kN)	Damage equivalent load Period (s)	(kN)		Ultimate load, F_U (kN)	
			$m = 4$	$m = 10$	$m = 4$	$m = 10$
No	11	1.7	2.6	6.7	458	47.7
Regular	1569	13.3	487	1182	43623	7164
Irregular	965	4.8	285	770	32851	5158

These cases include all cut off criteria, for both current velocity and significant wave height. Introducing either case of wave force increased the maximum ultimate load as seen in Table 5. The addition of the shear condition to the wave cases results in no change when compared with Table 3.

CONCLUSIONS

This paper presents an assessment of the influence of environmental conditions on load on a tidal stream turbine. The ultimate and damage equivalent loads of the tidal turbine components to withstand a design life of 10 years are assessed. A comparison between constant and variable turbulence intensity (TI) indicates that damage equivalent loads are greater for the higher constant turbulence intensities. Even if the mean TI for the variable case is used as a constant it would still over estimate. Therefore it is important to include the variation of TI throughout a tidal cycle when assessing damage equivalent loads. However all loads found for the affect of only including turbulence are greatly increased by the effect of waves. It has been confirmed that a the Morison type force formula is reasonably accurate for peak force due to regular waves, when compared to the experimental data. This is consistent with the relative form of the Morison equation that

is used for load cycles in irregular waves. These results show the influence of different environmental variables on the design parameters of a component for a target design life. Assuming regular waves the loads the component has to be designed for are higher than irregular waves by a factor of 1.5-2. As noted earlier in real sea states the waves will be irregular, therefore an assumption of regular waves would lead to over engineering of component to enable it to withstand much greater thrust forces than it would realistically experience.

FURTHER WORK

This study employed an approximate spectrum for turbulence loads based on reduced scale experimental data. Various studies have addressed turbulence simulation and turbulence loading to higher precision. Further investigation is required on the accuracy to which turbulence, and the resultant loading, should be synthesised to accurately assess design life. Wave period is from a fixed reference and so further analysis should account for Doppler shift of the wave-number, accounting for wave direction, the effect of current on wave height should also be considered. The case studied here concerns an isolated turbine with vertical shear of the onset flow velocity representative ambient conditions only causing load variation at the rotational frequency. For a turbine within an array onset flow may also be sheared in the horizontal plane due to the wake of upstream turbines and variation of flow through a turbine row. Wake turbulence will also differ from ambient turbulence and waves may be modified as they propagate over the wakes of turbine arrays thus the variation of unsteady loading within arrays requires further assessment.

ACKNOWLEDGMENTS

Thanks to Phillipe Gleizon (University of Highlands and Islands, Thurso) who provided the wave buoy data. Thanks to DNV-GL who provided a research license to allow the use of Tidal Bladed. The experiments conducted were part of the XMED project supported by funding from EPSRC (EP/J010235/1). The research conducted is supported by an EPSRC DTP studentship (EP/P117127) as well as a President's Doctoral Scholarship from The University of Manchester.

REFERENCES

Bianchi, F. D., De Battista, H., and Mantz, R. J. (2006). *Wind Turbine Control Systems*, volume 26.

Blackmore, T., Myers, L. E., and Bahaj, A. S. (2016). Effects of turbulence on tidal turbines: Implications to performance, blade loads, and condition monitoring. *International Journal of Marine Energy*, 14:1–26.

Chamorro, L. P., Hill, C., Morton, S., Ellis, C., Arndt, R. E. a., and Sotiropoulos, F. (2013). On the interaction between a turbulent open channel flow and an axial-flow turbine. *Journal of Fluid Mechanics*, 716:658–670.

DCNS (2016). Openhydro Deploys Second Paimpil-Brehat Turbine.

DNV-GL (2015). Standard Tidal Turbines (DNVGL-ST-0164). (October).

Downing, S. D. and Socie, D. F. (1982). Simple rainflow counting algorithms. *International Journal of Fatigue*, 4(1):31–40.

Elasha, F., Mba, D., Teixeira, J. A., and Togneri, M. (2015). Life Prediction of Tidal turbine Gearboxes. In *Proceedings of 11th European Wave and Tidal Energy Conference, Nantes, France*, pages 2–9.

European Commission (2016). State aid: Commission authorises French support for renewable tidal energy demonstration plant at Raz Blanchard. Technical report.

Fernandez-Rodriguez, E. (2015). *Analysis of Floating Support Structures for Marine and Wind Energy*. PhD thesis.

Fernandez-Rodriguez, E., Stallard, T. J., and Stansby, P. K. (2014). Experimental study of extreme thrust on a tidal stream rotor due to turbulent flow and with opposing waves. *Journal of Fluids and Structures*, 51:354–361.

Fleming, C., McIntosh, S., and Willden, R. (2013). Tidal turbine performance in sheared flow. *10th European Wave and Tidal Energy Conference*.

Freebury, G. and Musial, W. (2000). Determining equivalent damage loading for full-scale wind turbine blade fatigue tests. *2000 ASME Wind Energy Symposium*, (February):12.

Galloway, P. (2013). *Performance quantification of tidal turbines subjected to dynamic loading*. PhD thesis, University of Southampton.

Gaurier, B., Davies, P., Deuff, A., and Germain, G. (2013). Flume tank characterization of marine current turbine blade behaviour under current and wave loading. *Renewable Energy*, 59:1–12.

McCann, G. N. (2007). Tidal current turbine fatigue loading sensitivity to waves and turbulence a parametric study. *GH Tidal Bladed*.

Meygen (2017). Meygen: The Project.

Milne, I. a., Sharma, R. N., Flay, R. G. J., and Bickerton, S. (2010). The Role of Waves on Tidal Turbine Unsteady Blade Loading. In *3rd International Conference on Ocean Energy*, number 1, pages 1–6.

Morison, J., Johnson, J., and Schaaf, S. (1950). The Force Exerted by Surface Waves on PIles. *Journal of Petroleum Technology*, 2(5).

Mycek, P., Gaurier, B., Germain, G., Pinon, G., and Rivoalen, E. (2014). Experimental study of the turbulence intensity effects on marine current turbines behaviour. Part I: One single turbine. *Renewable Energy*, 66:729–746.

Natural Resources Canada (2016). Tidal Energy Project in the Bay of Fundy.

Parkinson, S. G. and Collier, W. J. (2016). Model validation of hydrodynamic loads and performance of a full-scale tidal turbine using Tidal Bladed. *International Journal of Marine Energy*, 16:279–297.

Sutherland, D. R. J., Sellar, B. G., and Bryden, I. (2012). The use of Doppler Sensor Arrays to Characterise Turbulence at Tidal Energy Sites. *ICOE proceedings*, pages 1–6.

Val, D. V. and Chernin, L. (2011). Probabilistic Evaluation of Failure Rates of Mechanical Components in Tidal Stream Turbines. *EWTEC 2011 Proceedings*.

Veers, P. (2009). *Fatigue loading of wind turbines*. Woodhead Publishing Limited.

View publication stats